Dynamics of the Cavity Generated in a Liquid Film by Drop Impact

M. Budakli[*1], T. Gambaryan-Roisman[1,3], S. Göhler[1], N. van Hinsberg[2], I. V. Roisman[2,3], P. Stephan[1,3] and C. Tropea[2,3]

[1]Chair of Technical Thermodynamics, Technische Universität Darmstadt
[2]Chair of Fluid Mechanics and Aerodynamics, Technische Universität Darmstadt
[3]Center of Smart Interfaces. Technische Universität Darmstadt
64287 Darmstadt, Germany

Abstract

The hydrodynamics of a drop impacting onto a liquid film are rather important when trying to understand and predict spray related processes like spray cooling or spray coating. The underlying physics essential for this understanding can be investigated well by examining a single drop impact onto a liquid film or layer, which is the subject of this study.

Drop impact onto a liquid layer generates an expanding cavity which penetrates into the layer due to inertia. In some cases, if the initial velocity exceeds the splash threshold, drop impact leads to the formation of the uprising crown-like sheet and splashes. In the case of relatively deep liquid layers, the cavity growth is decelerated by the gravity and surface tension. If the initial thickness of the liquid layer is comparable with the drop diameter, the cavity expansion is significantly influenced by the bottom wall effects. As the distance between the cavity and the rigid bottom decreases with time after impact, the cavity penetration is increasingly influenced and damped by viscous forces. The residual thickness of the liquid film between the cavity and the bottom is one of the main parameters determining the heat transfer associated with spray impact and is therefore an interesting parameter to predict. For a hydrophobic surface, the residual thickness could also determine the condition for the rewetting of the substrate.

The present study examines experimentally and theoretically the main geometrical parameters of the cavity, especially the residual, minimum film thickness. This thickness is much smaller than the drop initial diameter and the initial film thickness. Its determination experimentally is therefore a challenging task. In the experiments the shape of the penetrating cavity generated by drop impact is observed using a high-speed video system. Additionally, the thickness of the liquid layer between the cavity and the wall is monitored in time using an instrument based on chromatic confocal imaging (CHR optical sensor). Liquid properties, initial film thickness and drop impact parameters are varied in the experiments.

The theoretical model for the cavity penetration is developed accounting for gravity, surface tension and liquid inertia. The equation of motion of the cavity tip is obtained from the linear momentum balance equation and the evolution of the film thickness during the viscous stage is described. The theoretical predictions agree well with the experimental data.

Introduction

Numerous experimental and numerical investigations have been performed analyzing single drop impact to formulate appropriate models of spray systems, such as for spray cooling, painting, coating or airblast atomization. During the impact of a droplet on a dry, wetted, heated or unheated surfaces, a variety of fundamental hydrodynamic and, for hot surfaces, thermodynamic phenomena can be observed. These phenomena can be modeled in detail by applying different methods such as the diffuse-interface model or VOF in numerical simulations [1,2]. Validation data for such studies has been obtained by studying the influence of material and dynamic parameters on the spreading process, using both theoretical models and experiments [3,4,5,6]. Phenomena regarding boiling and cooling effects during a droplet impacting on a heated surface, have been described by the experimental results in [7,8], where high Weber numbers, different wall roughness values and various wall temperatures were used. However, most of the previous work has focused on detecting velocities of secondary droplets, deformation mechanisms,

[*]Corresponding author, budakli@ttd.tu-darmstadt.de

crown propagation and its break-up and cooling effectiveness by using different measurement techniques such as the phase Doppler technique or high-speed imaging.

In the experimental study [9] of drop impact onto a spherical target the evolution of the lamella thickness was measured using a high-speed video system. Such observations are possible only on a convex surface of the target since in this case the thicker rim region appearing at the edges of the lamella do not prevent observation of the film profile.

In comparison to these investigations, the present work concentrates on measuring the film thickness on a wetted target at the point of drop impact using a confocal chromatic sensor (CHR). The initial film thickness h_0 was varied over a range of 100 µm to 300 µm with a step size of 100 µm. Therefore the non-dimensional film thickness took the values $H = h_0 / d_d$ = 0.05, 0.1, and 0.15, using an average droplet diameter of d_d = 2.1 mm. Furthermore, by means of a fluorescence additive, the interaction between the drop liquid and the liquid layer has been observed from the bottom through a thin borosilicate glass plate (thickness 0.2 mm).

Experimental set-up and method

The experimental setup is shown in Figure 1. The point of drop impact is illuminated using a light source of 500 W while the visualization is performed using a Photron Fastcam SA-1 high-speed camera with a frame rate of 30 kfps. Two syringe units are used: one to generate the droplets falling vertically perpendicular onto the target and a second syringe to lubricate and control the initial film layer on the glass plate. With the movable syringe unit 1, the fall height h_d of the droplet can be changed from 50 mm to 1350 mm, which allows the impact velocity to be varied. Deionized water has been used as a liquid.

The glass plate of diameter 20 mm was used as a target and was chemically treated to be hydrophilic. 22 laser drilled holes in the glass plate, each of diameter 0.5mm, allow water to be supplied from below to control the liquid layer thickness. This system avoids mechanical disturbances of the hydrophilic layer and allows the film thickness to be finely adjusted using the syringe unit 2. The average droplet diameter d_d = 2.1mm was determined directly from the images, averaging over 10 droplets for each fall height. The drop velocity was estimated by analyzing its propagation just before impact.

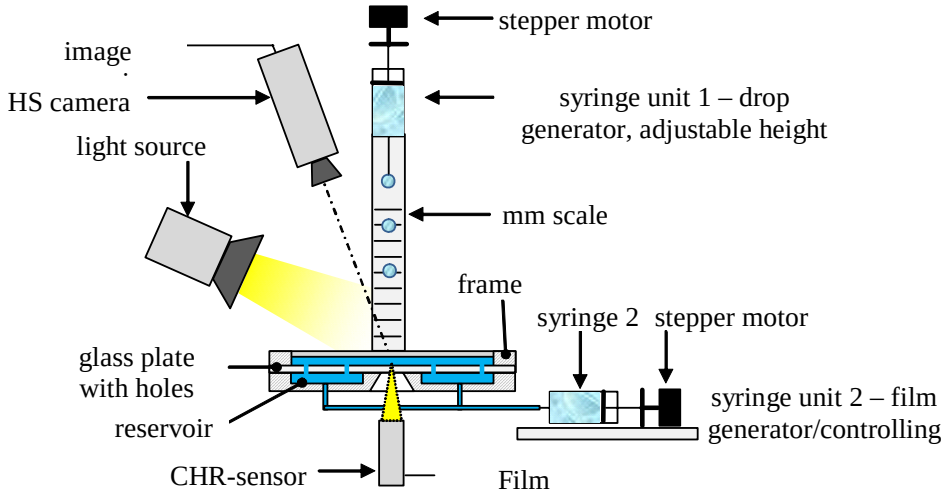

Figure 1. Experimental set-up.

To measure the film thickness $h_f(t)$ the CHR-sensor was positioned on the axis of the drop generator and the positioning was checked using preliminary images. After each impact the liquid layer relaxed to an undisturbed state for a minimum of about 10 seconds. The CHR-sensor sampled at 4 kHz over 6 seconds. Both the camera and the CHR sensor were synchronized and triggered from the computer.

Propagation of the cavity and evolution of the film thickness

For the thickness of the film under the crater created by drop impact, four typical regimes can be identified. In the first regime the film thickness reduces with almost constant velocity. It can be shown that this velocity is approximately half of the drop impact velocity [10]. The dimensionless penetration depth of the crater can be written in the form

$$y_{cr} = \frac{t}{2} \qquad \text{at} \quad t < 2 \tag{1}$$

where h_0 is the dimensionless unperturbed initial film thickness on the substrate. The equation is written in dimensionless form using the impact velocity as the velocity scale and the initial drop diameter as the length scale.

Next, at times $t > 2$ the drop is eroded completely and the cavity propagates and expands by inertial forces in the surrounding liquid. If the Weber and Reynolds numbers are high enough, the cavity propagation can be described well by the expansion of the spherical cavity. Neglecting the viscous and capillary effects, the flow past the propagating cavity can be assumed irrotational and the pressure field can be determined using the instationary Bernoulli equation. The pressure has to vanish at the cavity surface. This condition yields the evolution equation for the penetration depth of the cavity, the solution of which is obtained in the form

$$y_{cr} = 2^{-4/5}(5t-6)^{2/5} \qquad \text{at} \quad t > 2 \tag{2}$$

Next, when the cavity approaches the bottom of the liquid film its motion is influenced significantly by the wall. When the thickness of the liquid film between the cavity and rigid substrate is much smaller than the cavity diameter, the flow in this film can be described well by the remote asymptotic solution [11]. The thickness of the film at the impact axis is written in the following form:

$$h_f = \frac{\eta}{(t+\tau)^2} \tag{3}$$

The dimensionless constant coefficients τ and η in (3) are determined by the initial thickness of the unperturbed film. In the case of drop impact onto a dry wall these coefficients are $\tau = 0.25$ and $h = 0.25$, obtained from the numerical simulations in [12].

This theory is valid only in the time period when the film thickness is much thicker than the thickness of the viscous boundary layer appearing in the film immediately after impact. The self-similar analytical solution for the flow field in this boundary layer can be found in [13]. The dimensionless thickness of this layer can be estimated as

$$h_{BL} \approx 1.88\sqrt{t/\mathrm{Re}} \tag{4}$$

At the time instant $t = t_{BL}$ the boundary layer reaches the upper free surface of the film. Time instant t_{BL} can be easily estimated from the condition $h_{BL} = h_f$. At times $t > t_{BL}$ the film thickness is governed by the viscous effects which lead to the velocity deceleration and vanishing. The evolution equation in the viscous regime can be written in the form

$$\ddot{h}_f - \frac{9}{5}\frac{\dot{h}^2}{h} + \frac{3}{\mathrm{Re}}\frac{\dot{h}_f}{h_f^2} = 0 \tag{5}$$

the solution of which is

$$t = t_{BL} + \int \left[\left(V_0 + \frac{15}{14\,\mathrm{Re}\,h_0} \right) \frac{h^{9/5}}{h_0^{9/5}} - \frac{15}{14\,\mathrm{Re}\,h} \right]^{-1} dh \tag{6}$$

where V_0 is the rate of film thinning and h_0 is the film thickness at the time instant $t = t_{BL}$.
The expression for the residual film thickness is obtained in the form:

$$h_{res} = \frac{h_0^{9/14}}{\left(h_0^{-1} + 14/15\,\mathrm{Re}\,V_0\right)^{5/14}} \tag{7}$$

In the case of drop impact onto a dry substrate the theoretical predictions [13] for the residual film thickness are obtained in the following form

$$h_{res} \approx 0.79\,\mathrm{Re}^{-2/5} \tag{8}$$

It is obvious that the expression (8) is applicable also to the cases when the initial film thickness is much smaller than the initial drop diameter.

Results and discussion

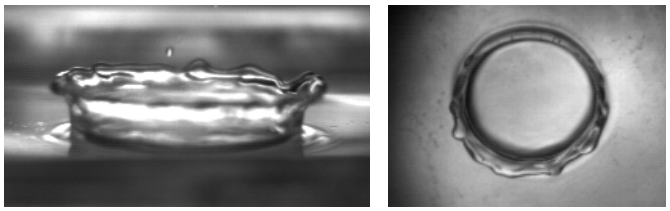

Figure 2. Drop impact on a liquid film with h_f = 200 µm, v_d = 2.4 m/s and d_d = 2 mm, side view (left), top view (right)

In Fig. 2 a drop impact on a thin liquid film is recorded from the side and top view with a high speed camera of a frequency of 4000 Hz. To determine the crown radius and the crown height, images are analyzed with a C++ code. As shown in figure 3 the crown radius and the crown height increases with increasing impact velocity of the droplet. Also with increasing We, the radial velocity of the crown expansion increases and a maximum crown diameter is reached earlier.

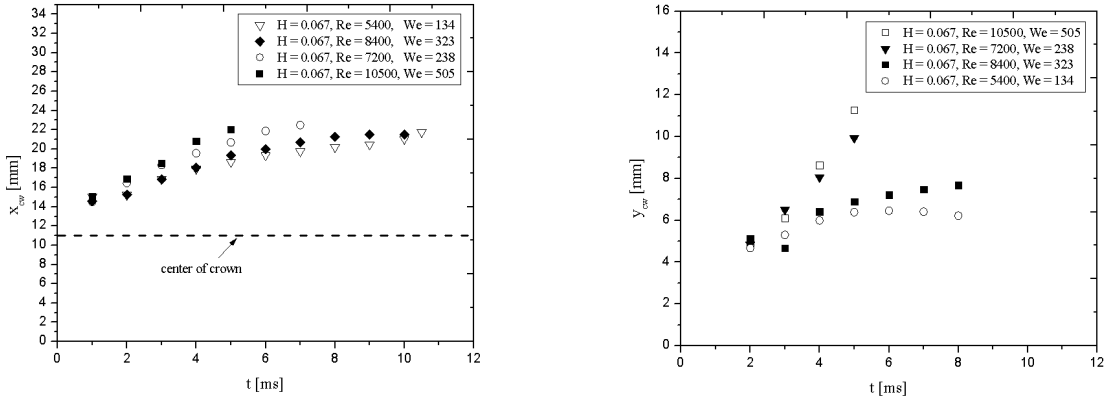

Figure 3. Crown radius (left) and crown height (right) of a liquid layer of the dimensionless film thickness H = 0.067

In Fig. 4 the asymptotic solutions for the penetration depth of the crater in a deep pool and in a finite liquid layer are compared with our experimental data and with the data from [14,15]. The agreement for the penetration into a deep pool is rather good for very high impact Weber and Froude numbers. If these parameters are relatively small, the crater motion is influenced by capillary forces. At some instant its penetration stops and the cavity starts to recede. It can also be seen that the presence of the substrate is significant, especially when the cavity approaches the rigid wall.

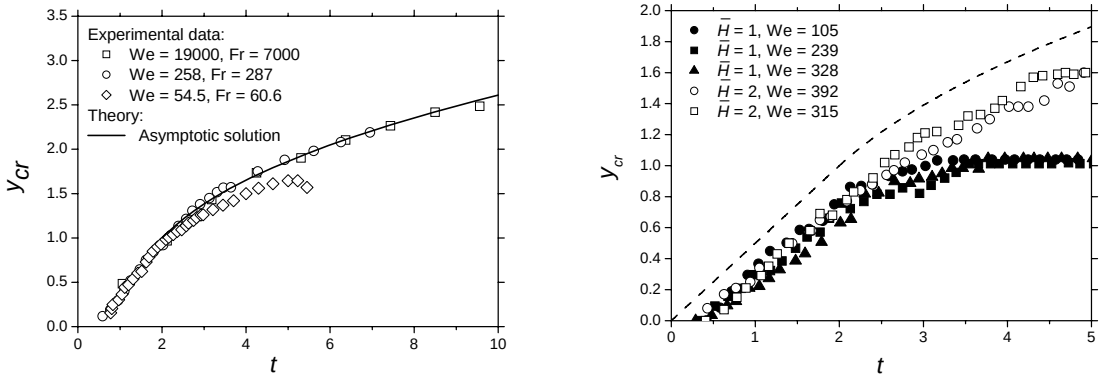

Figure 4. Penetration depth, y_{cr}, of a cavity into a deep pool (left) and into a liquid layer of the dimensionless film thickness $H = 1$ and $H = 2$ (right). The experiments for the drop impact onto a deep pool are from [14,15]. The theoretical predictions are given by (1)-(2).

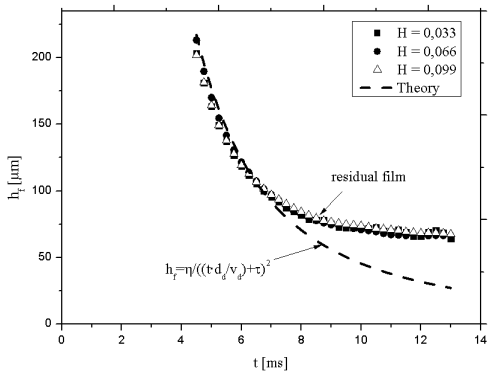

Figure 5. Film thickness in comparison with the theoretical predictions (3) for various initial film thicknesses. Re = 3780, We = 93.

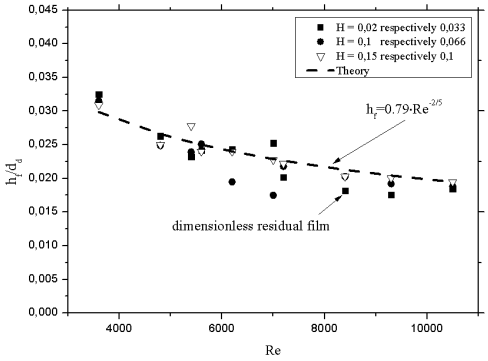

Figure 6. Dimensionless film thickness in comparison with the theoretical predictions for various initial film thickness and droplet diameter.

In Fig. 5 the results of measurements of the film thickness produced by drop impact onto liquid layers of various thicknesses are shown as a function of time. The exact instant of impact cannot be determined in our experiments since the drop diameter exceeds the upper value of the measurement range of the instrument. Nevertheless, the curves corresponding to various layer thicknesses lie approximately on one single curve. Two regions can be identified. One region (at $t < 7$ ms) can be well described by the remote asymptotic solution (3) and the second region corresponds to almost constant film velocity predicted by (6) (at times $t > 10$).

The results of the measurements of the residual film thickness are shown in Figure 6 as a function of the Reynolds number for three film thicknesses. Some scatter in the data is explained by the propagation of the capillary waves whose amplitude is comparable with the residual film thickness. The experimental data are compared with the theoretical expression (8). The agreement is rather good despite the fact that no adjustable parameters are used in the theory.

Conclusions

Drop impact onto a liquid film has been investigated experimentally and modeled theoretically. Four typical regimes are identified. Three regimes correspond to the inertia dominated flow while the fourth regime is influenced by viscosity. Viscous forces lead to the flow deceleration and to creation of the residual film of approximately constant thickness. If the Weber and Reynolds numbers are high the residual film thickness is a function solely of the Reynolds number. If the initial film thickness is much smaller than the initial drop diameter the theoretical expression developed for drop impact onto a dry substrate predicts well the value of the residual film thickness.

Acknowledgements

This study has been supported by the EU industrial project Nr. 571 00229 EXTICE. The authors would also like to thank the German Scientific Foundation (DFG) for financial support in the framework of the Collaborative Research Center 568 (TP A1 and A2), in the framework of research grant Nr. Tr. 194/34 and the Emmy Noether-Program.

Nomenclature

D	glass plate diameter
d_d	average droplet diameter
H	dimensionless film thickness
h_0	initial film thickness
h_{BL}	thickness of the viscous boundary layer
h_d	fall height of the droplet
h_f	film thickness
Re	Reynolds number, based on the drop impact velocity and diameter
t	time
V_0	rate of film thinning
We	Weber-number, based on the drop impact velocity and diameter
x_{cw}	crown radius
y_{cr}	dimensionless penetration depth of the crater
y_{cw}	crown height
η	dimensionless constant
τ	dimensionless constant

Subscripts

d	droplet
BL	boundary layer
f	film
cr	crater

References

1. Khatavkar, V.V., Anderson, P.D., Duineveld, P.C., and Meijer, H.E.H., *J. Fluid Mech.*, 581:97-127 (2007).
2. Fujimoto, H., Shiotani, Y., Tong, A.Y., Hama, H., Takuda, H., *Int. J.Multiphase Flow* 33: 317-332 (2007).
3. Rioboo, R., Marengo, M., Tropea, C., Exp. Fluids 33:112–124 (2002).
4. Roisman, I.V., Tropea, C., *J. Fluid Mech.*, 472:373-397 (2002).
5. Bejan, A., Gobin, D., Int. J. Heat Mass Transfer 49:2412–2419 (2006).
6. Mehdizadeh, N.Z., Chandra, S., Mostaghimi, J., *J. Fluid Mech.*, 510:353–373 (2004).
7. Akhtar, S.W., Yule, A.J., *ILASS 2001*, Zurich, September 2001.
8. Cossali, G.E., Marengo, M., Santini, M., *Exp. Therm. Fluid Sci*. 29:937–946 (2005).
9. Bakshi S., Roisman I. V., Tropea C., *Phys. Fluids*, 19, 032102 (2007).
10. Birkhoff, G., MacDougall, D. P., Pugh, E. M. and Taylor, G., *J. Appl. Phys.* 19: 563 (1948).
11. Yarin, A.L., Weiss, D.A., *J. Fluid Mech.* 283: 141–73 (1995).
12. Roisman, I.V. Berberovic, E. and Tropea, C. *Phys. Fluids*, 21, 052103 (2009)
13. Roisman, I.V. *Phys. Fluids*, 21, 052104 (2009)
14. Elmore, P. A., Chahine, G. L., Oguz, H. N., *Exp. Fluids*, 31:664-673 (2001).
15. Engel, O. G., *J. Appl. Phys.* 38, 3935 (1967).